Original Article

Protective Effect of Procyanidin B2 on Acute Liver Injury Induced by Aflatoxin B_1 in Rats*

DENG Zhi Jie[1], ZHAO Jing Fang[2], HUANG Feng[3], SUN Gui Li[1], GAO Wei[4,5], LU Li[4,5,#], and XIAO De Qiang[4,5,#]

1. Department of Clinical Nutrition, The Third Affiliated Hospital of Guangxi Medical University, Nanning 530031, Guangxi, China; 2. Department of Clinical Nutrition, Guangxi International Zhuang Medicine Hospital, Nanning 530000, Guangxi, China; 3. Department of Clinical Nutrition, Liuzhou General Hospital, Liuzhou 545006, Guangxi, China; 4. Department of Nutrition and Food Hygiene, School of Public Health, Guangxi Medical University, Nanning 530021, Guangxi, China; 5. Guangxi Colleges and Universities Key Laboratory of Prevention and Control of Highly Prevalent Diseases, Guangxi Medical University, Nanning 530021, Guangxi, China

Abstract

Objective This study aimed to explore the protective effect of procyanidin B2 (PCB2) on acute liver injury induced by aflatoxin B_1 (AFB_1) in rats.

Methods Forty Sprague Dawley rats were randomly divided into control, AFB_1, AFB_1 + PCB2, and PCB2 groups. The latter two groups were administrated PCB2 intragastrically (30 mg/kg body weight) for 7 d, whereas the control and AFB_1 groups were given the same dose of double distilled water intragastrically. On the sixth day of treatment, the AFB_1 and AFB_1 + PCB2 groups were intraperitoneally injected with AFB_1 (2 mg/kg). The control and PCB2 groups were intraperitoneally administered the same dose of dimethyl sulfoxide (DMSO). On the eighth day, all rats were euthanized: serum and liver tissue were isolated for further examination. Hepatic histological features were assessed by hematoxylin and eosin-stained sections. Weight, organ coefficient (liver, spleen, and kidney), liver function (serum alanine aminotransferase, aspartate aminotransferase, alkaline phosphatase, total bilirubin, and direct bilirubin), oxidative index (catalase, glutathione, superoxide dismutase, malondialdehyde, and 8-hydroxy-2′-deoxyguanosine), inflammation factor [hepatic interleukin-6 (IL-6) mRNA expression and serum IL-6], and bcl-2/bax ratio were measured.

Results AFB_1 significantly caused hepatic histopathological damage, abnormal liver function, oxidative stress, inflammation, and bcl-2/bax ratio reduction compared with DMSO-treated controls. Our results indicate that PCB2 treatment can partially reverse the adverse liver conditions induced by AFB_1.

Conclusion Our findings indicate that PCB2 exhibits a protective effect on acute liver injury induced by AFB_1.

Key words: Procyanidin B2; Aflatoxin B_1; Acute liver injury; Oxidative stress; Inflammation

Biomed Environ Sci, 2020; 33(4): 238-247 *doi: 10.3967/bes2020.033* *ISSN: 0895-3988*

www.besjournal.com (full text) *CN: 11-2816/Q*

*This work was financially supported by National Natural Science Foundation of China [No. 31360383].

#Correspondence should be addressed to LU Li, Tel: 86-771-5358259, E-mail: luligx@163.com; XIAO De Qiang, Tel: 86-771-5358259, E-mail: dak407@189.cn

Biographical note of the first author: DENG Zhi Jie, male, born in 1991, MD, majoring in clinical nutrition.

INTRODUCTION

Aflatoxin B_1 (AFB_1), a secondary metabolite produced mainly by fungi, *Aspergillus flavus* and *Aspergillus parasiticus*, is one of the most toxic carcinogens known to date[1]. Areas with warm, humid climates and abundant rain provide optimal growth conditions for these molds. Improper storage of food leads to AFB_1 contamination easily, and foods such as peanuts, corn, rice, sorghum, milk, and oil are susceptible to AFB_1 contamination[2]. Once the food is contaminated by AFB_1, it is difficult to remove it[3]. The exposure of AFB_1 due to contamination is difficult to be realized, resulting in hepatocellular carcinoma after a long-term process[4]. Therefore, it is necessary to develop effective methods to prevent AFB_1-induced hepatotoxicity.

In the mammalian body, the liver is the main target organ for AFB_1 toxicity. AFB_1 can be absorbed into the body through the skin, digestive tract, and respiratory tract. Upon entering the body, AFB_1 is mainly metabolized to AFB_1-exo-8, 9-epoxide (AFBO), aflatoxin M_1, and aflatoxicol by the cytochrome P450 enzyme system and cytoplasmic reductase enzymes in the liver[5]. AFBO, which binds to DNA resulting in the formation of AFB_1-DNA adducts, leads to mutations and carcinogenesis[6,7]. It has also been reported that AFB_1 can lead to liver injury *via* oxidative damage[8-10], inflammation[11], apoptosis[12].

Natural phytochemicals have gained great attraction for properties of chemical toxicity resistance by exerting multiple biological activities in recent years. Grape seed procyanidin extract (GSPE), rich in polyphenols, plays a protective role in liver injury induced by environmental toxicants, such as AFB_1[13], lead[14,15], and fluoride[16]. As one of the main components of GSPE, procyanidin B2 (PCB2) shows a similar positive impact on the liver. It is reported that PCB2 ameliorates acute hepatic injury and liver fibrosis caused by carbon tetrachloride (CCl_4)[17,18]. PCB2 has also been shown to reduce hepatic steatosis through transcription factor EB-mediated lysosomal and redox state[19]. Moreover, PCB2 protects against nonalcoholic fatty liver disease by modulating gut microbiota[20]. Taken together, these findings suggest that PCB2 exhibits a hepatoprotective effect, but whether PCB2 has a protective effect on AFB_1-induced acute liver injury remains unknown.

The present study aimed to determine the protective effect of PCB2 on acute liver injury induced by AFB_1 through *in vivo* experiments. The results of this study would lay a foundation for further research on the prevention of hepatocellular carcinoma and provide a theoretical basis for future dietary guidance to prevent the negative effects of AFB_1.

MATERIALS AND METHODS

Chemicals and Reagents

PCB2 [purity > 98.0% high-performance liquid chromatography (HPLC)] was purchased from Chengdu Biopurify Phytochemicals Ltd. (Chengdu, China). AFB_1 (purity > 98.0% HPLC) was purchased from Sigma Aldrich (USA). Dimethyl sulfoxide (DMSO, purity ≥ 99.9%) was purchased from MP Biomedicals (USA). Superoxide dismutase (SOD), catalase (CAT), glutathione (GSH), and malondialdehyde (MDA) assay kits were purchased from Nanjing Jiancheng Bioengineering Institute (Nanjing, China). Bicinchoninic acid (BCA) protein assay kit was purchased from MULTI SCIENCES (Hangzhou, China). Eastep® Super Total RNA Extraction Kit, GoScript™ Reverse Transcription Mix, and GoTaq® quantitative polymerase chain reaction (qPCR) Master Mix were purchased from Promega Corporation (USA). Interleukin-6 (IL-6) and 8-hydroxy-2'-deoxyguanosine (8-OHdG) enzyme-linked immunosorbent assay (ELISA) kits were purchased from Jiangsu Meimian Industrial Co., Ltd. (Jiangsu, China). Primary antibodies against bcl-2 and bax were purchased from Cell Santa Cruz Biotechnology (USA); the β-actin antibody was purchased from Cell Signaling Technology Inc. (USA). The secondary goat anti-rabbit and goat anti-mouse horseradish peroxidase-conjugated antibodies were purchased from Cell Signaling Technology Inc. Western Lightning Plus enhanced chemiluminescence (ECL) was purchased from PerkinElmer Inc. (USA).

Animals and Treatments

Six week-aged male Sprague Dawley (SD) rats were purchased from Guangxi Medical University Laboratory Animal Center (Nanning, China). All rats were housed in standard animal cages with free access to food and water under a strict 12 h light-dark cycle. They were acclimated to the animal facility environment for 1 week before experiments. SD rats were randomly divided into four groups (n = 10 each). The control and AFB_1 groups were given

double distilled water by gavage for 5 d consecutively. The AFB_1 + PCB2 and PCB2 groups were administered PBC2 by gavage for 5 consecutive days (30 mg/kg, dissolved in double distilled water). After 5 d of gavage, the AFB_1 and AFB_1 + PCB2 groups were given single intraperitoneal injections of AFB_1 (2 mg/kg, dissolved in DMSO) on the sixth day, whereas the control and PCB2 groups intraperitoneally received equal volume of DMSO. The AFB_1 + PCB2 and PCB2 groups received daily intragastric administration of PCB2, whereas the other two groups received daily intragastric administration of double distilled water continually until the end of experiment. On the eighth day, the animals were euthanized. Blood samples were collected, and the serum was separated immediately. The liver tissue was isolated from each rat, washed in ice-cold saline, and stored at −80 °C for further experimental analyses. The dose, administration way, and exposure time of AFB_1 mentioned earlier were based on study of Cui et al.[21] and Wang[22]. All experimental procedures were approved by the Animal Ethics Committee of Guangxi Medical University (Nanning, China). The whole procedure of animal treatment can be seen in Figure 1.

Measurement of Body Mass, Liver Coefficient, Spleen Coefficient, and Kidney Coefficient

The body mass of all rats were weighed at a fixed time every morning. The whole liver, spleen, and kidney were weighed after being isolated from body, rinsed by ice-cold saline, and dried by filter paper. Weight gain was calculated as body weight after experiment minus the body weight before experiment. Liver coefficient, spleen coefficient, and kidney coefficient were calculated as liver mass/body mass, spleen mass/body mass, and kidney mass/body mass, respectively. The calculation result was expressed as g/100 g.

Liver Function Determination

The whole blood remained still for 1 h at 4 °C after collection, and then, the serum was separated by centrifugation at 3,000 rpm for 15 min at 4 °C. Serum alanine aminotransferase (ALT), aspartate aminotransferase (AST), total bilirubin (TBIL), direct bilirubin (DBIL), and alkaline phosphatase (ALP) were detected by Hitachi 7600-020 automatic biochemical analyzer, following the manufacturer's protocol.

Hepatic Pathological Examination

The excised liver tissue was fully fixed in 4% paraformaldehyde and then dehydrated, paraffin-embedded, sectioned, and stained with hematoxylin and eosin. The sections of liver tissue were observed with EVOS FL Auto Cell Imaging System.

Measurement of Oxidative Stress

Liver tissue was homogenized in ice-cold saline at a ratio of 1:9 (g:mL) and centrifuged at 2,500 rpm for 10 min at 4 °C. The supernatant was used for hepatic CAT, GSH, and SOD detection. The serum was used to measure MDA concentration. The measurements were performed according to the manufacturer's instructions.

Determination of Serum IL-6 and Hepatic 8-OHdG

The serum level of interleukin-6 (IL-6) and hepatic level of 8-OHdG were measured by ELISA kits. Samples were prepared before performing ELISA test. For 8-OHdG determination, the required supernatant was obtained by homogenizing liver tissue in phosphate-buffered saline at a ratio of 1:9 (g:mL) and centrifuging at 5,000 rpm for 15 min. The serum was directly used to detect IL-6 concentration. The operation steps of ELISA include as follows: preparing standard solution for standard curve establishment, loading samples, washing plate, rendering color, terminating reaction, and

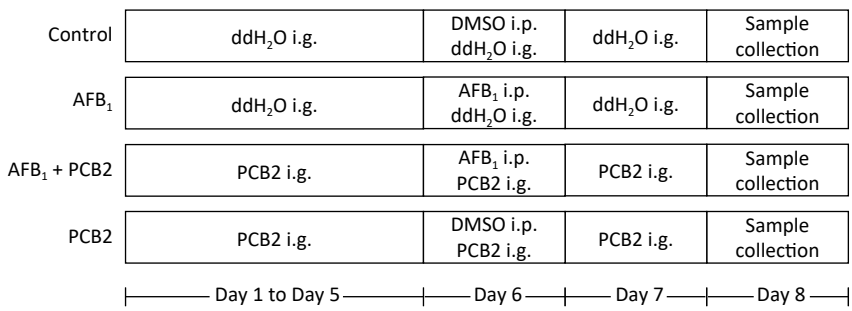

Figure 1. The procedure of animal treatment. i.p., intraperitoneal injection; i.g., intragastric; AFB_1, aflatoxin B_1; PCB2, procyanidin B2; DMSO, dimethyl sulfoxide.

determining the optical density value. All procedures were performed following the manufacturer's instructions of ELISA kits.

RNA Extraction and qPCR Analysis of IL-6 and bcl-2/bax Ratio

Total RNA was extracted from the liver tissue by Eastep® Super Total RNA Extraction Kit. RNA reverse transcription was conducted by GoScript™ Reverse Transcription Mix, and qPCR was performed using GoTaq® qPCR Master Mix. The primers used in this study are listed in Table 1. PCR amplification was carried out by StepOne™ Real-Time PCR System for 40 cycles; the procedures included prevariation at 95 °C for 10 min, denaturation at 95 °C for 15 s, annealiation at 55 °C for 30 s, and extension at 72 °C for 30 s.

Western Blotting Analysis of bcl-2/bax Ratio

The excised liver tissue was homogenized in RIPA lysis buffer [1% Triton X-100, 1% deoxycholate, 0.1% sodium dodecylsulphate (SDS), and 1 mmol/L phenylmethylsulfonyl fluoride]. The lysate was centrifuged at 14,000 g for 10 min. The supernatant was used for protein quantification by BCA protein assay kit to ensure equal loading of total protein of each sample on a 12% SDS-polyacrylamide gel electrophoresis gel. The proteins were transferred to polyvinylidene fluoride membranes. Membranes were incubated with blocking buffer (20% skim milk) for 30 min at room temperature and then incubated with primary antibodies for bcl-2, bax, and β-actin overnight at 4 °C. Subsequently, the membranes were washed three times using 1× Tris-buffered saline with Tween buffer and incubated with secondary antibodies for 1 h at room temperature. The proteins on membrane were visualized by Western Lightning Plus ECL. The intensity of each protein band was quantified by densitometry using Image J software[23].

Table 1. Polymerase chain reaction primers and the amplified product length

Gene	Primer sequences (5'-3')	Product length (bp)
IL-6	Forward: AGTTGCCTTCTTGGGACTGA Reverse: CCTCCGACTTGTGAAGTGGT	126
bcl-2	Forward: GACTGAGTACCTGAACCGGCATC Reverse: CTGAGCAGCGTCTTCAGAGACA	135
bax	Forward: AGACACCTGAGCTGACCTTGGA Reverse: TTGAAGTTGCCATCAGCAAACA	196
β-actin	Forward: GGAGATTACTGCCCTGGCTCCTA Reverse: GACTCATCGTACTCCTGCTTGCTG	150

Statistical Analysis

All data were expressed as mean ± standard deviation. Data were analyzed by one-way analysis of variance and followed by a least significant difference test. Statistical analysis was performed using SPSS 20.0 software. $P < 0.05$ was identified as statistically different.

RESULTS

PCB2 Reduced Abnormal AFB_1-induced Organ Coefficient

The liver, spleen, and kidney index coefficients were elevated in rats exposed to AFB_1 compared with the control group (all $P < 0.01$). PCB2 lowered the liver and kidney coefficients in AFB_1-treated rats (all $P < 0.01$). The weight gain was inhibited by AFB_1 ($P < 0.01$), while PCB2 could not significantly prevent it as shown in the AFB_1 + PCB2 group *versus* the AFB_1 group ($P > 0.05$; Figure 2A–D).

PCB2 Ameliorated AFB_1-induced Hepatic Histopathological Damage

Histopathological change of liver sections was performed under the life EVOS FL Auto Cell Imaging System. The control and PCB2 groups showed normal liver architecture with even texture and polygonal hepatocytes. Liver injury in the AFB_1 group was characterized by rough texture, spotty necrosis, ballooning degeneration of liver cells, and inflammatory cell infiltration, whereas the AFB_1 + PCB2 group showed a reduction in these negative histopathological changes. The result indicated that the administration of PCB2 might have a protective effect on AFB_1-induced histopathological damage (Figure 3A–D).

PCB2 Reduced Abnormal Liver Function Caused by AFB_1

After exposure to AFB_1, rats exhibited higher serum levels of ALT, AST, TBIL, DBIL, and ALP (all $P < 0.01$). PCB2 treatment decreased the serum levels of ALT, AST, TBIL, DBIL, and ALP (all $P < 0.05$); however, the levels detected were still above baseline (all $P < 0.01$). There was no statistical difference between the control and PCB2 groups (all $P > 0.05$). The results suggest that PCB2 could ameliorate AFB_1-induced liver damage (Figure 3E–I).

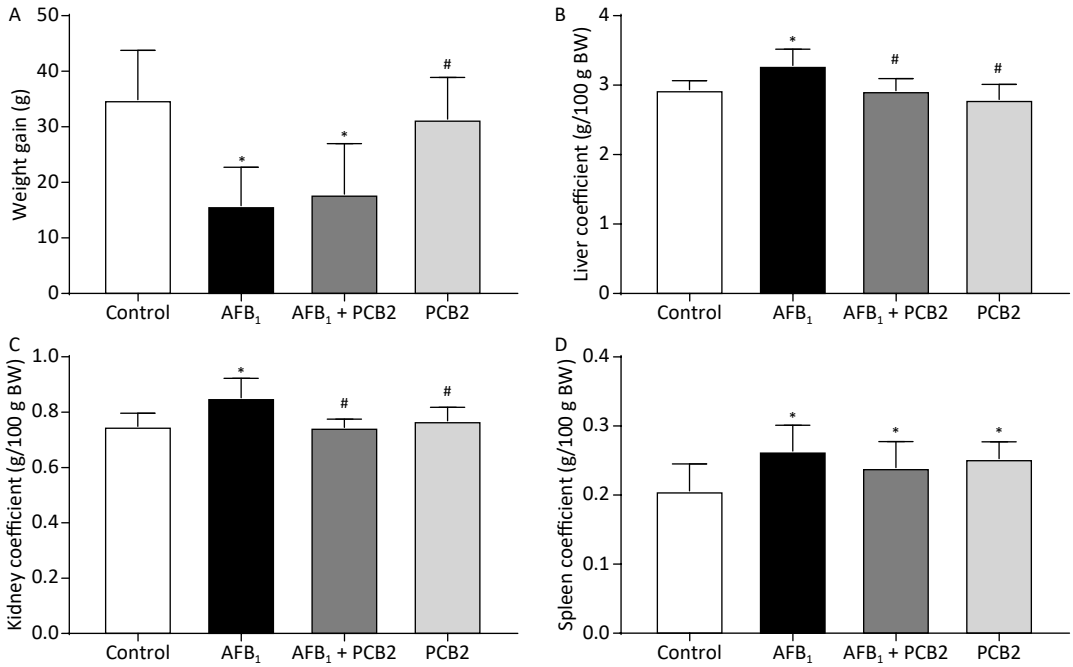

Figure 2. PCB2 reduced the abnormal AFB_1-induced organ coefficient. (A) Total weight gain during the experiment, (B) liver coefficient, (C) kidney coefficient, and (D) spleen coefficient. The data are expressed as mean ± standard deviation. $^{*}P < 0.05$ *vs.* the control group; $^{\#}P < 0.05$ *vs.* the AFB_1 group. SD, standard deviation; AFB_1, aflatoxin B_1; PCB2, procyanidin B2.

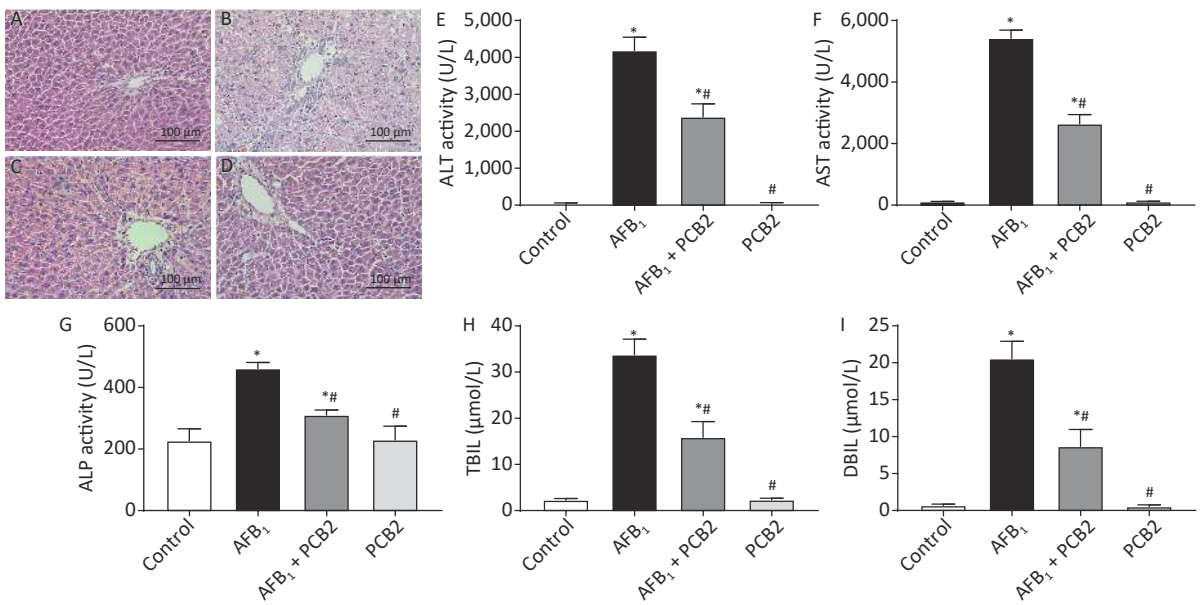

Figure 3. Procyanidin B2 (PCB2) ameliorated aflatoxin B_1 (AFB_1)-induced hepatic histopathological damage and abnormal liver function. Hematoxylin and eosin staining of the liver in the (A) control group, (B) AFB_1 group, (C) AFB_1 + PCB2 group, and (D) PCB2 group. (E) Serum alanine aminotransferase (ALT), (F) aspartate aminotransferase (AST), (G) alkaline phosphatase (ALP) activities, (H) total bilirubin (TBIL), and (I) direct bilirubin (DBIL) were measured. Scale bars: 100 μm. The data are expressed as mean ± standard deviation. $^{*}P < 0.05$ *vs.* the control group; $^{\#}P < 0.05$ *vs.* the AFB_1 group.

PCB2 Suppressed AFB$_1$-induced Oxidative Injury

Hepatic activities of CAT, SOD, GSH, 8-OHdG, and serum MDA were measured to access the extent of oxidation. CAT, GSH, and SOD levels were decreased in the AFB$_1$ group compared with that in the control group (all $P < 0.01$), whereas the MDA and 8-OHdG levels were increased in the AFB$_1$ group compared with that in the control group (both $P < 0.01$). PCB2 treatment could significantly reverse the decreased CAT, GSH, and SOD levels (all $P < 0.05$) and increased MDA and 8-OHdG levels as shown in the AFB$_1$ + PCB2 group versus the AFB$_1$ group ($P < 0.01$ or $P < 0.05$). The oxidative extent between the control and PCB2 groups was comparable (all $P > 0.05$). Since 8-OHdG is the biomarker of DNA oxidative damage, the results indicate that PCB2 could prevent the oxidative injury of liver tissue and DNA oxidative damage caused by AFB$_1$ (Figure 4A–E).

PCB2 Inhibited AFB$_1$-induced Inflammatory Response

AFB$_1$ treatment significantly increased hepatic IL-6 mRNA expression and serum IL-6 compared with the control group ($P < 0.05$ or $P < 0.01$), whereas PCB2 treatment decreased the expression and levels of these two inflammatory response markers compared with the AFB$_1$ group ($P < 0.05$ or $P < 0.01$). There was no significant difference between the control and PCB2 groups in IL-6 mRNA expression and serum levels of IL-6 (both $P > 0.05$). The results hinted that PCB2 could hinder inflammatory response induced by AFB$_1$ (Figure 4F and G).

PCB2 Decreased AFB$_1$-induced Apoptosis of Hepatocytes

The mRNA and protein ratios of bcl-2/bax suggest apoptosis of hepatocytes. When the ratio decreases, it indicates that hepatocytes may undergo apoptosis. Compared with the control group, the mRNA and protein ratios of bcl-2/bax were significantly lower in the AFB$_1$ group (both $P < 0.01$). However, the mRNA and protein bcl-2/bax ratios were higher in the AFB$_1$ + PCB2 group than the AFB$_1$ group ($P < 0.01$ or $P < 0.05$). The mRNA and protein bcl-2/bax ratios in the PCB2 group were

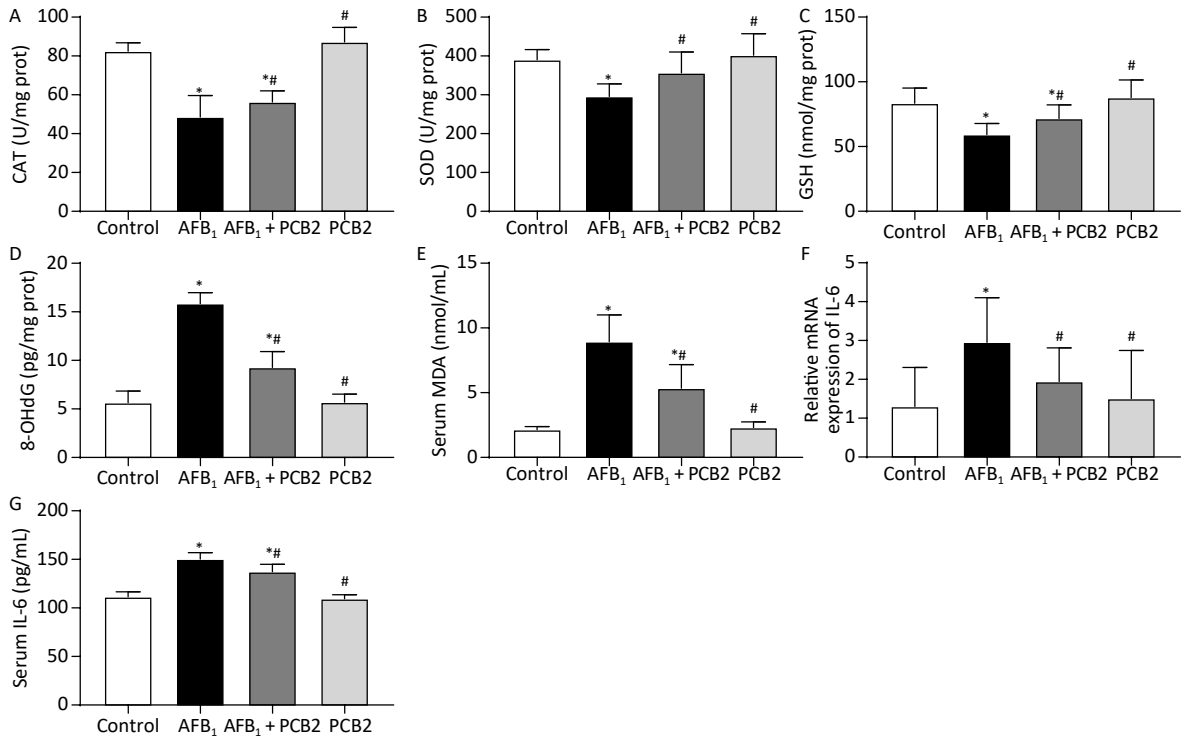

Figure 4. Procyanidin B2 (PCB2) suppressed aflatoxin B$_1$ (AFB$_1$)-induced oxidative injury and inflammatory response. (A) Hepatic catalase (CAT) activity, (B) hepatic superoxide dismutase (SOD) activity, (C) hepatic glutathione (GSH) content, (D) hepatic 8-hydroxy-2'-deoxyguanosine (8-OHdG) content, (E) serum malondialdehyde (MDA) content, (F) relative mRNA expression of IL-6, and (G) serum interleukin-6 (IL-6) concentration. The data are expressed as mean ± standard deviation. $^{*}P < 0.05$ *vs.* the control group; $^{\#}P < 0.05$ *vs.* the AFB$_1$ group.

comparable with those in the control group (both $P > 0.05$). The results revealed that PCB2 might decrease AFB_1-induced apoptosis of hepatocytes (Figure 5A–G).

DISCUSSION

AFB_1 has been classified as a group 1 carcinogen, which is the top level of carcinogenicity categories, by the International Agency for Research on Cancer recently[24]. Previous studies have shown that AFB_1 exerts carcinogenesis after being transformed into intermediate metabolites[3]. Meanwhile, the formation of AFBO and reactive oxygen species (ROS) deplete GSH, resulting in oxidative stress[5]. Histopathological change, liver dysfunction, and inflammation always exist in AFB_1-induced hepatotoxicity[25-27]. In this study, PCB2 significantly ameliorated these adverse effects, which may partially explain its protective properties on AFB_1-induced liver injury.

The organ coefficient is the ratio of organ mass to body weight, which reflects the influence of a substance on experimental animals. Changes in body weight and organ mass during the course of an experiment can affect the organ coefficient. In this study, the weight gain of the AFB_1 group rats was lower than that of the control group, whereas the liver, spleen, and kidney coefficients were higher (Figure 2A–D), indicating that body weight change is one of the main factors affecting the organ coefficient of rats subjected to acute liver injury. Previous studies have also shown that AFB_1 has a negative effect on weight gain[28,29], probably due to the impaired liver function affecting appetite and biosynthesis. Compared with the AFB_1 group, there was no significant change in the weight gain of the AFB_1 + PCB2 group, but the liver and kidney coefficients decreased (Figure 2A–C), suggesting that PCB2 may reduce the abnormal weight gain of liver and kidney caused by AFB_1.

Histopathological examination is the gold standard for determining hepatic damage. Once a liver injury occurs, hepatocytes may undergo edema, necrosis or apoptosis, and inflammatory cell infiltration[30]. AFB_1 was reported to cause

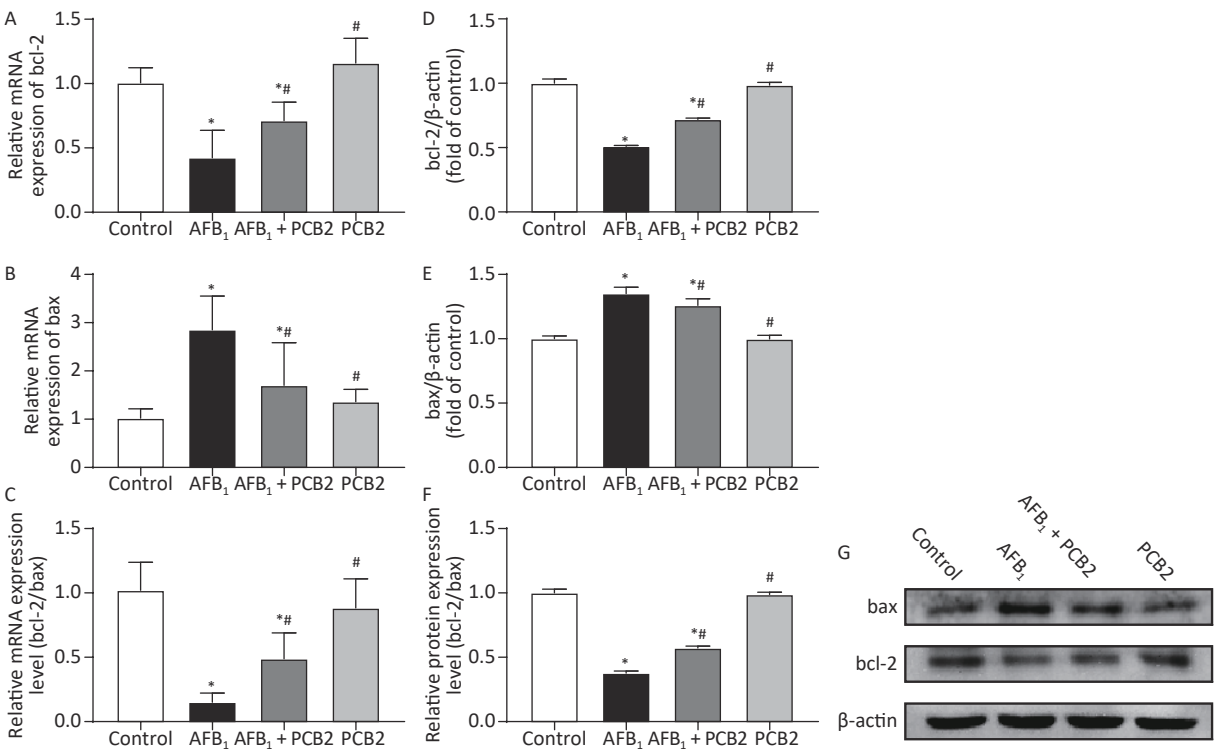

Figure 5. Procyanidin B2 (PCB2) decreased aflatoxin B_1 (AFB_1)-induced apoptosis of hepatocytes. Relative mRNA expression of (A) bcl-2, (B) bax, and (C) bcl-2/bax mRNA ratio were measured. Western blot analysis of (D) bcl-2, (E) bax, and (F) bcl-2/bax protein ratio were performed. (G) Protein strip of bax, bcl-2, and β-actin. The data are expressed as mean ± standard deviation. $^{*}P < 0.05$ *vs.* the control group; $^{\#}P < 0.05$ *vs.* the AFB_1 group.

acute liver injury at an intraperitoneal injection dose of 1.5 mg/kg, characterized by the structure of hepatic lobule becoming abnormal, hepatocytes showing a balloon-like change, and bile duct hyperplasia in the portal area accompanied by inflammatory cell infiltration[31]. In our study, the pathological damage of liver tissue was observed 48 h after exposure to 2 mg/kg AFB_1 in SD rats. The hepatocytes showed obvious balloon-like changes; the hepatic cord structure was destroyed; the texture of the tissue was disordered, and there were spotted necrosis and inflammatory cell infiltration (Figure 3B), which was similar to previous studies. While the clearer structure of liver tissue could be seen in the AFB_1 + PCB2 group (Figure 3C), this finding indicates that PCB2 has a protective effect on AFB_1-induced hepatic pathological damage.

Intracellular ALT, AST, and ALP are released into the peripheral blood, increasing the concentration of these enzymes in the serum when hepatocytes undergo damage. In addition, the ability of hepatocyte to ingest, transform, and excrete bilirubin is reduced, resulting in elevating levels of serum bilirubin[32,33]. Therefore, serum ALT, AST, ALP, and bilirubin can serve as biomarkers of liver dysfunction. It was reported that when rats were exposed to AFB_1, serum ALT, AST, and TBIL increased[34,35]. The current study showed that the serum ALT, AST, ALP, TBIL, and DBIL of rats were elevated after the exposure to AFB_1, whereas PCB2 administration could reduce these five indexes (Figure 3E–I), suggesting that PCB2 could ameliorate liver dysfunction.

GSH, CAT, and SOD are proteins or enzymes that scavenge oxygen free radicals and toxins in the body. GSH, composed of glutamate, cysteine, and glycine, is the main antioxidant of the human body exerting a detoxification effect[36]. SOD is an essential antioxidant enzyme widely found in living organisms, which catalyzes the disproportionation of superoxide anion to oxygen and hydrogen peroxide[37]. CAT is the enzyme that catalyzes the decomposition of hydrogen peroxide[38]. The concentration of these proteins or enzymes serves as a surrogate measure of the body's ability to resist oxidative damage. MDA is the end product of lipid peroxidation, which reflects the degree of lipid peroxidation damage in the body[39]. 8-OHdG is the biomarker of DNA oxidative damage, mainly caused by ROS attacking the eighth carbon atom of the guanine base in DNA[40]. Oxidative damage induced by AFB_1 can be monitored by detecting SOD, CAT, MDA, and 8-OHdG[41,42]. Our study found that AFB_1 leads to obvious oxidative damage with descending GSH, CAT, and SOD and elevating 8-OHdG and MDA, whereas PCB2 administration could inversely change the tendency (Figure 4A–E). Therefore, PCB2 may have a protective effect on AFB_1-induced oxidative damage.

When inflammation occurs in the body, the immune system secretes a large number of cytokines into the blood, leading to an increasing concentration of these factors in the serum[43,44]. Previous studies showed that AFB_1 could promote inflammation *via* elevating the levels of interleukin-1β (IL-1β), IL-6, and tumor necrosis factor-α and involving the activated nuclear factor kappa B (NF-κB) signaling pathways by upregulation of toll-like receptor 2 (TLR2) and TLR4[45,46]. IL-6 is an important pro-inflammatory factor mediating the acute inflammatory response and inducing B/T cell proliferation[47]. In our research, relative IL-6 mRNA expression and serum IL-6 levels increased in the AFB_1 group compared with that of in the control group. Conversely, PCB2 treatment could decrease IL-6 gene expression and serum IL-6 level (Figure 4F and G). Long et al.[48] and Hinton et al.[49] observed that AFB_1 treatment led to increased serum IL-6, whereas GSPE could lower the concentration of IL-6[48], which was similar to our findings. These results indicated that PCB2 could alleviate the inflammatory response caused by AFB_1, but the underlying mechanism needs further research.

Bcl-2 and bax are proteins regulating the initiation of apoptosis. When the ratio of bcl-2/bax protein expression decreases, cells are more likely to undergo apoptosis[50]. Apoptosis is a biological process of programmed cell death[51]. According to previous studies, AFB_1 invokes apoptosis in the process of exerting hepatotoxicity, which upregulation of p53, caspase-3, and bax and downregulation of bcl-2 can be measured[52]. Meanwhile, the apoptosis induced by AFB_1 is related to the death receptor pathway[12] and the Nrf2 signal pathway[53]. In this study, the gene and protein expression of bcl-2 in single AFB_1-treated rats decreased (Figure 5A–D), whereas the gene and protein expressions of bax increased (Figure 5B and E), resulting in a decreased bcl-2/bax ratio (Figure 5C and F). Compared with AFB_1-treated rats, the gene and protein expressions of bcl-2 in PCB2 + AFB_1 rats increased (Figure 5A and D), bax expression decreased (Figure 5B and E), and bcl-2/bax ratio increased (Figure 5C and F). It is speculated that AFB_1 may cause apoptosis during the process of inducing

acute liver injury; PCB2 could inhibit liver damage by reducing hepatocyte apoptosis. Terminal deoxynucleotidyl transferase-mediated dUTP nick-end labeling assay is a better method to detect tissue apoptosis[54,55], thus, it would be better to apply it for further research.

GSPE has been proven to display a protective effect on AFB_1-induced toxicity. Administration of GSPE was found to attenuate hepatotoxicity, immunotoxicity, and oxidative stress caused by AFB_1 via modulating NF-κB and Nrf2 pathways, which restored liver dysfunction and contents of antioxidant enzymes and inhibited mRNA expression of inflammatory factors[13,46,48]. Although these findings indicate that GSPE may be a potent substance resistant to AFB_1 toxicity, it remains unknown which components play the main role, for GSPE is a mixture of procyanidins. In this study, we observed that PBC2, one of the main components of GSPE, reduced serum AST, ALT, MDA, and IL-6 and elevated hepatic CAT, GSH, and SOD under the acute exposure of AFB_1, exhibiting the similar characteristics of GSPE. Previous studies also showed that PCB2 exerted hepatoprotective effect through anti-oxidation and anti-inflammatory on liver injury induced by chemical substances like CCl_4[17,18]. In summary, PCB2 may protect against toxicant-induced liver damage mainly targeting oxidation and inflammation, while the mechanisms of which need further exploration.

In conclusion, this study reveals that PCB2 has an inhibitory effect on AFB_1-induced acute liver injury, mainly in reducing histopathological damage, oxidative damage, inflammation, and probable apoptosis in hepatocytes. Therefore, PCB2 may serve as a potential phytochemical with anti-AFB_1 toxicity. However, this study does not explore the dose-effect relationship between PCB2 and AFB_1. Further research needs to be conducted to address this relationship.

CONFLICT OF INTEREST

The authors declared no conflict of interests.

AUTHOR CONTRIBUTIONS

DENG Zhi Ji and ZHAO Jing Fang conducted most experiments, DENG Zhi Jie wrote the paper; HUANG Feng assisted in the completion of animal experiments; SUN Gui Li and GAO Wei collected the experiment data; LU Li and XIAO De Qiang designed this study, LU Li revised this paper.

Received: October 24, 2019;
Accepted: February 5, 2020

REFERENCES

1. Kowalska A, Walkiewicz K, Koziel P, et al. Aflatoxins: characteristics and impact on human health. Postepy Hig Med Dosw (Online), 2017; 71, 315−27.
2. Medina A, Rodriguez A, Magan N. Effect of climate change on *Aspergillus flavus* and aflatoxin B1 production. Front Microbiol, 2014; 5, 348.
3. Rushing BR, Selim MI. Aflatoxin B1: a review on metabolism, toxicity, occurrence in food, occupational exposure, and detoxification methods. Food Chem Toxicol, 2019; 124, 81−100.
4. Nugraha A, Khotimah K, Rietjens I. Risk assessment of aflatoxin B1 exposure from maize and peanut consumption in Indonesia using the margin of exposure and liver cancer risk estimation approaches. Food Chem Toxicol, 2018; 113, 134−44.
5. Bbosa GS, Kitya D, Odda J, et al. Aflatoxins metabolism, effects on epigenetic mechanisms and their role in carcinogenesis. Health, 2013; 10, 720−6.
6. Eaton DL, Gallagher EP. Mechanisms of aflatoxin carcinogenesis. Annu Rev Pharmacol Toxicol, 1994; 34, 135−72.
7. Engin AB, Engin A. DNA damage checkpoint response to aflatoxin B1. Environ Toxicol Pharmacol, 2019; 65, 90−6.
8. Shen HM, Shi CY, Lee HP, et al. Aflatoxin B1-induced lipid peroxidation in rat liver. Toxicol Appl Pharmacol, 1994; 127, 145−50.
9. Qiu T, Shen X, Li X, et al. Egg yolk immunoglobulin supplementation prevents rat liver from aflatoxin b1-induced oxidative damage and genotoxicity. J Agric Food Chem, 2018; 66, 13260−7.
10. El-Nekeety AA, Salman AS, Hathout AS, et al. Evaluation of the bioactive extract of actinomyces isolated from the Egyptian environment against aflatoxin B1-induce cytotoxicity, genotoxicity and oxidative stress in the liver of rats. Food Chem Toxicol, 2017; 105, 241−55.
11. Ma Q, Li Y, Fan Y, et al. Molecular mechanisms of lipoic acid protection against aflatoxin b1-induced liver oxidative damage and inflammatory responses in broilers. Toxins (Basel), 2015; 7, 5435−47.
12. Mughal MJ, Xi P, Yi Z, et al. Aflatoxin B1 invokes apoptosis via death receptor pathway in hepatocytes. Oncotarget, 2017; 8, 8239−49.
13. Ali Rajput S, Sun L, Zhang N, et al. Ameliorative effects of grape seed proanthocyanidin extract on growth performance, immune function, antioxidant capacity, biochemical constituents, liver histopathology and aflatoxin residues in broilers exposed to aflatoxin b_1 [published correction appears in Toxins (Basel). 2018 Sep 10;10(9)]. Toxins (Basel), 2017; 9, 371.
14. Yang D, Jiang H, Lu J, et al. Dietary grape seed proanthocyanidin extract regulates metabolic disturbance in rat liver exposed to lead associated with PPARα signaling pathway. Environ Pollut, 2018; 237, 377−87.
15. Liu B, Jiang H, Lu J, et al. Grape seed procyanidin extract ameliorates lead-induced liver injury via miRNA153 and AKT/GSK-3β/Fyn-mediated Nrf2 activation. J Nutr Biochem, 2018; 52, 115−23.
16. Niu Q, He P, Xu S, et al. Fluoride-induced iron overload contributes to hepatic oxidative damage in mouse and the protective role of grape seed proanthocyanidin extract. J Toxicol Sci, 2018; 43, 311−9.

17. Yang BY, Zhang XY, Guan SW, et al. Protective effect of procyanidin B2 against CCl4-induced acute liver injury in mice. Molecules, 2015; 20, 12250–65.
18. Wang Z, Zhang Z, Du N, et al. Hepatoprotective effects of grape seed Procyanidin B2 in rats with carbon tetrachloride-induced hepatic fibrosis. Altern Ther Health Med, 2015; 21(Suppl 2), 12–21.
19. Su H, Li Y, Hu D, et al. Procyanidin B2 ameliorates free fatty acids-induced hepatic steatosis through regulating TFEB-mediated lysosomal pathway and redox state. Free Radic Biol Med, 2018; 126, 269–86.
20. Xing YW, Lei GT, Wu QH, et al. Procyanidin B2 protects against diet-induced obesity and non-alcoholic fatty liver disease via the modulation of the gut microbiota in rabbits. World J Gastroenterol, 2019; 25, 955–66.
21. Cui Y, Ling JG, Yao WR, et al. Protective Effect of Aloe vera against Aflatoxin B1-Induced Acute Hepatotoxicity in Rats. Food Sci, 2016; 37, 175–81. (In Chinese)
22. Wang HJ, Wu ZB. Histological, histochemical and ultrastructural studies on acute hepatic injury induced by aflatoxin b1 in rats. J Tongji Med Univ, 1992; 153–5, 211. (In Chinese)
23. Schneider CA, Rasband WS, Eliceiri KW. NIH Image to ImageJ: 25 years of image analysis. Nat Methods, 2012; 9, 671–5.
24. IARC monographs preamble–preamble to the IARC ponographs (amended January 2019). WHO. https://monographs.iarc.fr/iarc-monographs-preamble-preamble-to-the-iarc-monographs/. [2019-9-11]
25. Muhammad I, Wang X, Li S, et al. Curcumin confers hepatoprotection against AFB1-induced toxicity *via* activating autophagy and ameliorating inflammation involving Nrf2/HO-1 signaling pathway. Mol Biol Rep, 2018; 45, 1775–85.
26. Yılmaz S, Kaya E, Comakli S. Vitamin E (α tocopherol) attenuates toxicity and oxidative stress induced by aflatoxin in rats. Adv Clin Exp Med, 2017; 26, 907–17.
27. Qian G, Tang L, Lin S, et al. Sequential dietary exposure to aflatoxin B1 and fumonisin B1 in F344 rats increases liver preneoplastic changes indicative of a synergistic interaction. Food Chem Toxicol, 2016; 95, 188–95.
28. Amaya-Farfan J. Aflatoxin B1-induced hepatic steatosis: role of carbonyl compounds and active diols on steatogenesis. Lancet, 1999; 353, 747–8.
29. Solis-Cruz B, Hernandez-Patlan D, Petrone VM, et al. Evaluation of a bacillus-based direct-fed microbial on aflatoxin b1 toxic effects, performance, immunologic status, and serum biochemical parameters in broiler chickens. Avian Dis, 2019; 63, 659–69.
30. Kleiner DE. Histopathological challenges in suspected drug-induced liver injury. Liver Int, 2018; 38, 198–209.
31. Shyamal S, Latha PG, Suja SR, et al. Hepatoprotective effect of three herbal extracts on aflatoxin B1-intoxicated rat liver. Singapore Med J, 2010; 51, 326–31.
32. Dufour DR, Lott JA, Nolte FS, et al. Diagnosis and monitoring of hepatic injury. I. Performance characteristics of laboratory tests. Clin Chem, 2000; 46, 2027–49.
33. Dufour DR, Lott JA, Nolte FS, et al. Diagnosis and monitoring of hepatic injury. II. Recommendations for use of laboratory tests in screening, diagnosis, and monitoring. Clin Chem, 2000; 46, 2050–68.
34. Brinda R, Vijayanandraj S, Uma D, et al. Role of Adhatoda vasica (L.) Nees leaf extract in the prevention of aflatoxin-induced toxicity in Wistar rats. J Sci Food Agric, 2013; 93, 2743–8.
35. Ajiboye TO, Yakubu MT, Oladiji AT. Lophirones B and C prevent aflatoxin B1-induced oxidative stress and DNA fragmentation in rat hepatocytes. Pharm Biol, 2016; 54, 1962–70.
36. Berndt C, Lillig CH. Glutathione, glutaredoxins, and iron. Antioxid Redox Signal, 2017; 27, 1235–51.
37. Bowling AC, Schulz JB, Brown RH Jr, et al. Superoxide dismutase activity, oxidative damage, and mitochondrial energy metabolism in familial and sporadic amyotrophic lateral sclerosis. J Neurochem, 1993; 61, 2322–5.
38. Heck DE, Shakarjian M, Kim HD, et al. Mechanisms of oxidant generation by catalase. Ann N Y Acad Sci, 2010; 1203, 120–5.
39. Tsikas D. Assessment of lipid peroxidation by measuring malondialdehyde (MDA) and relatives in biological samples: Analytical and biological challenges. Anal Biochem, 2017; 524, 13–30.
40. Kasai H. What causes human cancer? Approaches from the chemistry of DNA damage. Genes Environ, 2016; 38, 19.
41. Kim YS, Kim YH, Noh JR, et al. Protective effect of korean red ginseng against aflatoxin b1-Induced hepatotoxicity in rat. J Ginseng Res, 2011; 35, 243–9.
42. Shen HM, Ong CN, Lee BL, et al. Aflatoxin B1-induced 8-hydroxydeoxyguanosine formation in rat hepatic DNA. Carcinogenesis, 1995; 16, 419–22.
43. Yao X, Huang J, Zhong H, et al. Targeting interleukin-6 in inflammatory autoimmune diseases and cancers. Pharmacol Ther, 2014; 141, 125–39.
44. Rose-John S. IL-6 trans-signaling via the soluble IL-6 receptor: importance for the pro-inflammatory activities of IL-6. Int J Biol Sci, 2012; 8, 1237–47.
45. Huang L, Zhao Z, Duan C, et al. Lactobacillus plantarum C88 protects against aflatoxin B1-induced liver injury in mice via inhibition of NF-κB-mediated inflammatory responses and excessive apoptosis. BMC Microbiol, 2019; 19, 170.
46. Rajput SA, Sun L, Zhang NY, et al. Grape seed proanthocyanidin extract alleviates aflatoxin b_1-induced immunotoxicity and oxidative stress *via* modulation of NF-κB and Nrf2 signaling pathways in broilers. Toxins (Basel), 2019; 11, 23.
47. Mosser DM, Edwards JP. Exploring the full spectrum of macrophage activation. Nat Rev Immunol, 2008; 8, 958–69.
48. Long M, Zhang Y, Li P, et al. Intervention of grape seed Proanthocyanidin extract on the subchronic immune injury in mice induced by aflatoxin b1. Int J Mol Sci, 2016; 17, 516.
49. Hinton DM, Myers MJ, Raybourne RA, et al. Immunotoxicity of aflatoxin B1 in rats: effects on lymphocytes and the inflammatory response in a chronic intermittent dosing study. Toxicol Sci, 2003; 73, 362–77.
50. Reed JC. Proapoptotic multidomain Bcl-2/Bax-family proteins: mechanisms, physiological roles, and therapeutic opportunities. Cell Death Differ, 2006; 13, 1378–86.
51. Elmore S. Apoptosis: a review of programmed cell death. Toxicol Pathol, 2007; 35, 495–516.
52. Wang X, Muhammad I, Sun X, et al. Protective role of curcumin in ameliorating AFB1-induced apoptosis via mitochondrial pathway in liver cells. Mol Biol Rep, 2018; 45, 881–91.
53. Liu Y, Wang W. Aflatoxin B1 impairs mitochondrial functions, activates ROS generation, induces apoptosis and involves Nrf2 signal pathway in primary broiler hepatocytes. Anim Sci J, 2016; 87, 1490–500.
54. Majtnerová P, Roušar T. An overview of apoptosis assays detecting DNA fragmentation. Mol Biol Rep, 2018; 45, 1469–78.
55. Loo DT. In situ detection of apoptosis by the TUNEL assay: an overview of techniques. Methods Mol Biol, 2011; 682, 3–13.